A Random Boolean Network Model
and Deterministic Chaos

Mihaela T. Matache*
Jack Heidel

Department of Mathematics

University of Nebraska at Omaha

Omaha, NE 68182-0243, USA

*dmatache@mail.unomaha.edu

Abstract This paper considers a simple Boolean network with N nodes, each node's state at time t being determined by a certain number of parent nodes, which may vary from one node to another. This is an extension of a model studied by Andrecut and Ali ([5]) who consider the same number of parents for all nodes. We make use of the same Boolean rule as the authors of [5], provide a generalization of the formula for the probability of finding a node in state 1 at a time t and use simulation methods to generate consecutive states of the network for both the real system and the model. The results match well. We study the dynamics of the model through sensitivity of the orbits to initial values, bifurcation diagrams, and fixed point analysis. We show that the route to chaos is due to a cascade of period-doubling bifurcations which turn into reversed (period - halving) bifurcations for certain combinations of parameter values.
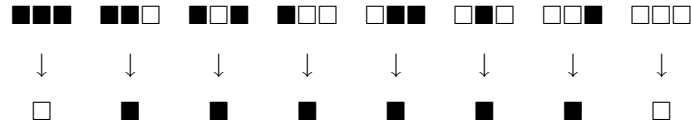
1. INTRODUCTION

In recent years various studies ([5], [16], [19], [20], [21], [22], [30], [31]) have shown that a large class of biological networks and cellular automata can be modelled as Boolean networks. These models, besides being easy to understand, are relatively easy to handle. The interest for Boolean networks and their applications in biology and automata networks has actually started much earlier ([8], [13], [14], [15], [25], [29], [32]), with publications such as the one of Kauffman ([25]) whose work on the self-organization and adaptation in complex systems has inspired many other research endeavors. At the same time it has been observed ([1], [6]) that large complex networks (biological, social, www) exhibit a scale-free feature, that is their connectivity distributions have a power-law form. It is important to understand and study the dynamics of Boolean networks in order to use them for simulation and prediction of the real networks they model.

There is a close connection between Boolean networks and cellular automata. Each consists of a set of nodes operated on by other nodes. For cellular automata there are an infinite number of nodes and they have a spatial structure. Boolean networks have only a finite number of nodes but they are not arranged in any spatial structure. Also cellular automata have the same up-date rule at each node while for Boolean networks the up-date rule can vary from one node to another.
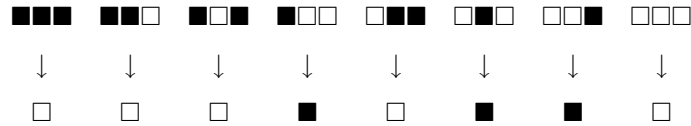
The present work is a significant generalization of previous work by Andrecut and Ali ([5]) which in turn generalizes rule 126 for elementary cellular automata ([38]). Rule 126 is one of several which exhibit randomly distributed triangular shapes of arbitrarily large size. This makes rule 126 a class III of complexity generating rule ([38]). The purpose of [5] is to show that this class III behavior has a simple interpretation as a density function for a random Boolean network exhibiting deterministic chaos. But we pause briefly to discuss Rule 126 itself.

Rule 126, most simply described as

$$\begin{array}{cccccccc} \blacksquare\blacksquare\blacksquare & \blacksquare\blacksquare\square & \blacksquare\square\blacksquare & \blacksquare\square\square & \square\blacksquare\blacksquare & \square\blacksquare\square & \square\square\blacksquare & \square\square\square \\ \downarrow & \downarrow & \downarrow & \downarrow & \downarrow & \downarrow & \downarrow & \downarrow \\ \square & \blacksquare & \blacksquare & \blacksquare & \blacksquare & \blacksquare & \blacksquare & \square \end{array}$$

where black is ON and white is OFF, has an important role amongst the $256 = 2^8$ elementary cellular automata, those with two states, ON and OFF, and neighborhood of size 3. Rule 126 is both "legal", reflection symmetric with $(0,0,0) \rightarrow 0$, and "totalistic", where the rule depends only on the relative number of ON and OFF states and not their order ([37]). There are 32 legal rules, and 16 totalistic rules. Only 8 of these rules, including Rule 126, are in both classes. These eight thereby distinguished rules are # 0, 22, 104, 126, 128, 150, 232, 254. They separate into Wolfram's four classes as: Class I: 0, 128, 254; Class II: 104, 232; Class III: 22, 126, 150; Class IV: none. Besides the automata in Class I and Class II which have relatively simple behavior ([38]), this leaves only three: # 22, 126, and 150. But # 150 is additive (linear in algebraic form) which simplifies its analysis by transferring unusual effects from the structure of the automata to the initial conditions only.

Let us look at the structure of Rule 22:

$$\begin{array}{cccccccc} \blacksquare\blacksquare\blacksquare & \blacksquare\blacksquare\square & \blacksquare\square\blacksquare & \blacksquare\square\square & \square\blacksquare\blacksquare & \square\blacksquare\square & \square\square\blacksquare & \square\square\square \\ \downarrow & \downarrow & \downarrow & \downarrow & \downarrow & \downarrow & \downarrow & \downarrow \\ \square & \square & \square & \blacksquare & \square & \blacksquare & \blacksquare & \square \end{array}$$

As well as Rule 22 and Rule 126 both being in Wolfram's Class III, they are also both in the same $\kappa = 2$ in a new classification, regarding separating planes for the basic 8 point hypercube (along with # 104) ([10]).

It is interesting that both Rule 126 and Rule 22 have a natural and simple interpretation in terms of the growth of cell colonies. For Rule 126, complete crowding of live, ON, cells causes death, OFF, in the

next generation. Complete isolation of a potential cell prevents birth in the next generation. A similar interpretation holds for Rule 22, it just isn't quite as complete. It would be natural to try to extend what follows to a generalized Boolean network based on Rule 22. We have not yet figured out how to do this. See also [9].

The purpose of this discussion of Rule 126 is to provide the flavor for the general type of behavior which is analyzed in what follows. Although we will be discussing random Boolean networks, it is worthwhile to look briefly at the simplest nontrivial analogue in terms of a deterministic cellular automata.

In the paper [5] the authors consider a simple Boolean network with N nodes, each node being influenced by exactly k other nodes at each step of the Boolean system. In other words each node has exactly k parents, so that the Boolean rule for each node is determined only by the state of the k parents. The number k is fixed. This feature makes the model restrictive. It is known that in real networks the number of parents of a given node varies from one node to another. In this paper we extend that model by allowing different number of parents per node. We make use of the same Boolean rule as the authors of [5], namely if a node of the network and all its parents have the same value (0 or 1) at time t, then the value of the node at the next time step $t + 1$ is 0; otherwise it is 1. We provide a generalization of the formula for the probability of finding a node in state 1 at a time t in Section 2. The formula for the probability $p(t + 1)$ that a node is in state 1 at time $t + 1$ given $p(t)$ is

$$p(t+1) = \sum_{j=1}^{J} \frac{M_j}{N} \left[1 - \frac{N_0^{k_j}(t)}{M_j}(1 - p(t))^{k_j} - \frac{N_1^{k_j}(t)}{M_j} p(t)^{k_j} \right]$$

where N is the size of the network, $k_1, k_2, \ldots, k_J$ the distinct values for the number of parents of the nodes, M_j the number of nodes with k_j parents, $N_0^{k_j}$ the number of nodes with k_j parents that are in state 0, and $N_1^{k_j}$ the number of nodes with k_j parents that are in state 1. We use simulation methods to generate consecutive states of the network for both the real system and the model. The results match very well. In Section 3 we study the dynamics of the model through the analysis of the sensitivity of the orbits to the initial values, bifurcation diagrams, and fixed points. We show that the route to chaos is due to a cascade of period-doubling bifurcations which turn into reversed bifurcations for certain combinations of parameter values. The reversed bifurcations are explained in more detail in Section 4. As is shown here, a single large value for one of the k_j, can have a dramatic effect in simplifying the behavior of the rest of the network. Section 5 is dedicated to conclusions and possibilities for future work.

2. The Boolean Network Model

In this section we describe the Boolean model. Significant results from [5] are recalled to make the paper self-contained.

Consider a network with N nodes. Each node c_n, $n = 1, 2, \ldots, N$ can take on only two values 1 or 0. Often this is interpreted as a system in which each node can be either ON of OFF. At each time point

t the system can be in one of the 2^N possible states. We assume that all the nodes update their value at the same time, that is the network is synchronous. The evolution of the nodes from time t to time $t+1$ is given by a Boolean rule which is considered the same for all nodes. Each node c_n is assigned a random "neighborhood" of parents, whose values at time t influence the value of c_n at time $t+1$ through the following Boolean rule. If $c_n(t)$ and all its parents have the same value at time t (that is they are all either 0 or 1), then $c_n(t+1) = 0$, otherwise $c_n(t+1) = 1$. The parents of a node are chosen randomly from the remaining $N-1$ nodes and do not change thereafter. More precisely, if a node has k parents, then a set of k nodes is chosen from the remaining $N-1$ nodes with probability $\frac{1}{\binom{N-1}{k}}$.

This model is a description of a random Boolean cellular automaton. The system is described by the number of parents of each node. Observe that the quantity

$$N_1(t) := \sum_{n=1}^{N} c_n(t)$$

gives the number of cells that are in state 1 at time t. The concentration of nodes in state 1 is given by $\frac{1}{N}\sum_{n=1}^{N} c_n(t)$. We are interested in finding the probability $p(t+1)$ that a node is in state 1 at time $t+1$. In the paper [5] the authors show that $p(t+1)$ is given by

$$(2.1) \qquad p(t+1) = 1 - p(t)^{k+1} - (1 - p(t))^{k+1}$$

where $k \geq 1$ is the number of parents of each node (considered fixed in that paper). (Note: we take the liberty to provide the formula with $k+1$ rather than k as it is misprinted in [5]).

Our goal is to provide a similar formula for the case of variable number of parents. To this aim we start by making the following notations. Let $k_1, k_2, \ldots, k_J$ be the distinct values for the number of parents the nodes $c_1, c_2, \ldots, c_N$ can have. Also let C_j be the collection of all nodes having k_j parents, and M_j be the number of nodes in each class C_j, $j = 1, 2, \ldots, J$. To simplify the notation we will assume that $C_1 = \{c_1, c_2, \ldots, c_{M_1}\}$, $C_2 = \{c_{M_1+1}, c_{M_1+2}, \ldots, c_{M_1+M_2}\}$ and so on. Also, let $N_0^{k_j}(t)$ be number of nodes of class C_j in state 0 at time t, and $N_1^{k_j}(t)$ the number of nodes of class C_j in state 1 at time t, $j = 1, 2, \ldots, J$. It follows that $\sum_{j=1}^{J}(N_0^{k_j}(t) + N_1^{k_j}(t)) = N$, and $N_0^{k_j} + N_1^{k_j} = M_j$, $j = 1, 2, \ldots, J$. The probability that a node is in state 1 at time t is given by $p(t) = \frac{1}{N}\sum_{j=1}^{J} N_1^{k_j}(t)$. We want to compute the conditional probability that a node is in state 1 at $t+1$, given the known probability $p(t)$. Observe that this is basically determined by the number of nodes that change from state 0 at time t to state 1 at time $t+1$ and the number of nodes that remain in state 1 from time t to $t+1$.

We will start with the derivation of $N_{0\to1}^{k_j}(t)$ which will denote the number of nodes of class C_j that are 0 at time t and become 1 at time $t+1$. We will use the notation $\mathbf{P}$ for the probability of an event, but we will keep the notation $p(t)$ for the probability of a node being in state 1 at time t throughout the paper. If $c_n(t) = 0$ then

$$\mathbf{P}(c_n(t+1) = 1 | c_n(t) = 0) = \mathbf{P}(\text{at least one of the parents of node } c_n \text{ is 1 at time } t) =$$

$$= 1 - \mathbf{P}(\text{all parents of node } c_n \text{ are } 0 \text{ at time } t) = 1 - (1 - p(t))^k.$$

Here k denotes the number of parents of the node c_n and could be any of the numbers $k_1, k_2, \ldots, k_J$. We assume independence of the parents, in other words, the parents themselves can be in state 0 or 1 independently of each other. At time $t+1$ we could have $0, 1, 2, \ldots,$ or $N_0^{k_j}(t)$ nodes going from state 0 at time t to state 1 at $t+1$. We define the discrete random variable X given by the probability distribution function

$$\mathbf{P}(X = l) = \mathbf{P}(l \text{ nodes of class } C_j \text{ go from state } 0 \text{ at time } t \text{ to state } 1 \text{ at time } t + 1) =$$

$$= \binom{N_0^{k_j}(t)}{l} \left[1 - (1 - p(t))^{k_j}\right]^l \left[(1 - p(t))^{k_j}\right]^{N_0^{k_j}(t) - l}, \qquad l = 0, 1, 2, \ldots, N_0^{k_j}(t).$$

One can check by a straightforward computation that $\sum_{l=0}^{N_0^{k_j}(t)} \mathbf{P}(X = l) = 1$. Then $N_{0 \to 1}^{k_j}(t)$ will be the expected value of X, that is

$$(2.2) \qquad N_{0 \to 1}^{k_j}(t) = \sum_{l=0}^{N_0^{k_j}(t)} l\, \mathbf{P}(X = l) = N_0^{k_j}(t) \left[1 - (1 - p(t))^{k_j}\right].$$

Although this number might not be an integer, we will not make any adjustments given that our final goal is to compute a probability, which is anyway a number between 0 and 1. It is important to note that if the number of parents is the same for all nodes, say k, then $k_j = k$, for all $j = 1, 2, \ldots, J$ and the total number of nodes going from state 0 at time t to state 1 at time $t + 1$ is given by

$$N_{0 \to 1}(t) = N_0(t) \left(1 - (1 - p(t))^k\right), \qquad N_0(t) = \sum_{j=1}^{J} N_0^{k_j}(t).$$

This represents exactly the formula obtained in [5] for $N_{0 \to 1}(t)$.

By a similar argument, one can write the following formulas for $N_{1 \to 1}^{k_j}(t)$, the number of nodes of class C_j that remain 1 from time t to $t + 1$, $N_{0 \to 0}^{k_j}(t)$ the number of nodes of class C_j that remain 0, and $N_{1 \to 0}^{k_j}(t)$, the number of nodes of class C_j that change from 1 to 0. In each case an appropriate random variable is defined as above, and the number of nodes going from one state at time t to the next state at time $t + 1$ is defined as the expected value of that random variable. Thus we obtain the following:

$$N_{1 \to 1}^{k_j}(t) = N_1^{k_j}(t)(1 - p(t)^{k_j}), \quad N_{0 \to 0}^{k_j}(t) = N_0^{k_j}(t)(1 - p(t))^{k_j}, \quad \text{and} \quad N_{1 \to 0}^{k_j}(t) = N_1^{k_j}(t)p(t)^{k_j}.$$

Again, by setting all numbers k_j equal to k and performing the computations we get the formulas obtained in [5], namely

$$N_{1 \to 1}(t) = N_1(t)(1 - p(t)^k), \quad N_{0 \to 0}(t) = N_0(t)(1 - p(t))^k, \quad \text{and} \quad N_{1 \to 0}(t) = N_1(t)p(t)^k$$

where $N_0(t) = \sum_{j=1}^{J} N_0^{k_j}(t), N_1(t) = \sum_{j=1}^{J} N_1^{k_j}(t)$.

It is important to check that the sum of all these quantities is equal to N.

Remark *The following holds*

$$N_{0\to1}(t) + N_{1\to1}(t) + N_{0\to0}(t) + N_{1\to0}(t) = N.$$

Proof. Observe that $N_{0\to1}^{k_j}(t) + N_{0\to0}^{k_j}(t) = N_0^{k_j}(t)$, $j = 1, 2, \ldots, J$. Similarly, observe that $N_{1\to1}^{k_j}(t) + N_{1\to0}^{k_j}(t) = N_1^{k_j}(t)$, $j = 1, 2, \ldots, J$. These results are to be expected and they immediately imply that $N_{0\to1}(t) + N_{1\to1}(t) + N_{0\to0}(t) + N_{1\to0}(t) = N$.

$\square$

We can now construct the quantities $p_j(t+1) = \frac{1}{N}\left[N_{0\to1}^{k_j}(t) + N_{1\to1}^{k_j}(t)\right]$ where $j = 1, 2, \ldots, J$, representing the probabilities of finding a node of class C_j in state 1 at time $t+1$. Observe that

$$p_j(t+1) = \frac{M_j}{N} - \frac{N_0^{k_j}(t)}{N}(1-p(t))^{k_j} - \frac{N_1^{k_j}(t)}{N}p(t)^{k_j} = \frac{M_j}{N}\left[1 - \frac{N_0^{k_j}(t)}{M_j}(1-p(t))^{k_j} - \frac{N_1^{k_j}(t)}{M_j}p(t)^{k_j}\right].$$

The quantities $\frac{N_0^{k_j}(t)}{M_j}$ and $\frac{N_1^{k_j}(t)}{M_j}$ represent the proportion of nodes of class C_j that are 0, respectively 1, at time t. Thus we can write the final formula for the probability that a node is in state 1 at time $t+1$

$$(2.3) \qquad p(t+1) = \sum_{j=1}^{J} p_j(t+1) = \sum_{j=1}^{J} \frac{M_j}{N}\left[1 - \frac{N_0^{k_j}(t)}{M_j}(1-p(t))^{k_j} - \frac{N_1^{k_j}(t)}{M_j}p(t)^{k_j}\right].$$

Note that if all the nodes are 0 at time t, then $N_0^{k_j}(t) = N, N_1^{k_j}(t) = 0$, for all $j = 1, 2, \ldots J$, so that $p(t+1) = 0$, which is to be expected since by the Boolean rule all the nodes stay 0 at time $t+1$. Similarly, if all the nodes are 1 at time t, $p(t+1) = 0$ by the formula, as well as by the Boolean rule.

Given all of the above, we propose the following simulation algorithm for the Boolean network under consideration. The algorithm provides the computation of $p(t)$ for all $t = 0, 1, 2, \ldots$.

- For $t = 0$ choose arbitrary numbers $p_j(0) \in [0, \frac{M_j}{N}]$, $j = 1, 2, \ldots, J$, and let

$$p(0) = \sum_{j=1}^{J} p_j(0).$$

- For each $t = 0, 1, 2, \ldots$ compute

$$p_j(t+1) = \frac{M_j}{N}\left[1 - \left(1 - \frac{p_j(t)}{\frac{M_j}{N}}\right)(1-p(t))^{k_j} - \frac{p_j(t)}{\frac{M_j}{N}}p(t)^{k_j}\right] =$$

$$(2.4) \qquad = \frac{M_j}{N}\left[1 - (1-p(t))^{k_j} + \frac{p_j(t)}{\frac{M_j}{N}}\left((1-p(t))^{k_j} - p(t)^{k_j}\right)\right]$$

where $j = 1, 2, \ldots, J$, and let

$$p(t+1) = \sum_{j=1}^{J} p_j(t).$$

The formula for $p_j(t)$ in (2.4) is similar to the summands for $p_j(t)$ in (2.3).

It is useful to provide some simulations to see how well does the model match the real system. Of course, we will be able to provide visual output only for the case when $J = 2$, that is we only have 2 possible number of parents for each node. The simulations that follow in this paper have been obtained by running Matlab and Maple programs. The next graphs (Figure 1) represent simulations of the model and the actual Boolean system when $k_1 = 4, k_2 = 16, \frac{M_1}{N} = \frac{M_2}{N} = \frac{1}{2}$. Figure 1 represents the first four iterations of the model and the system, that is $p(t+1)$, respectively $p(t+2), p(t+3), p(t+4)$ versus $p_1(t)$ and $p_2(t)$. For the model we obtain surfaces that are graphed as a mesh, while for the simulated Boolean system we obtain only isolated points, generalizing figure 1 in [5].
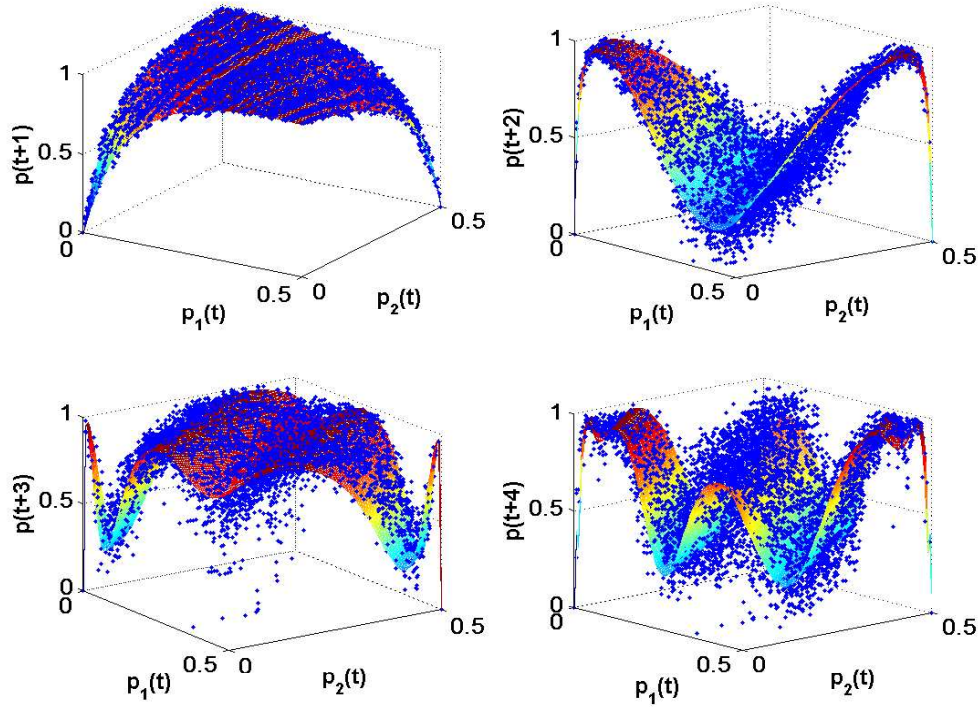
FIGURE 1. Simulation of the Boolean system and the model. The four graphs are the first four iterations, representing $p(t + 1), p(t + 2), p(t + 3), p(t + 4)$ respectively, versus $p_1(t)$ and $p_2(t)$. In all the figures, the number of nodes is $N = 160$, the proportion of nodes with $k_1 = 4$ parents is $\frac{M_1}{N} = \frac{1}{2}$, and the proportion of nodes with $k_2 = 16$ parents is $\frac{M_2}{N} = \frac{1}{2}$. The iterations of the system are graphed with points, whereas the iterations of the model are surfaces graphed as a mesh.

As one can see, although there is no perfect match, the model is a very good approximation for the Boolean system. We note that the graphs are few of many simulations run by the authors for various parameter combinations. The results of the simulations were always similar to the ones in the graphs of Figure 1. The running time for the program is rather long due to complex computations. Therefore

we kept the number of nodes at a reasonable magnitude (160 in the graphs mentioned above). But the larger the number of nodes, the better the match between the model and the Boolean system.

In the next section we are interested in studying the dynamics of a system governed by the rules in the model (2.3).

3. Model Dynamics

We point out to begin with that the dynamics of higher dimensional analogues of [5] may be quite compatible with the one dimensional behavior [5], p. 21, as illustrated in Figure 2.
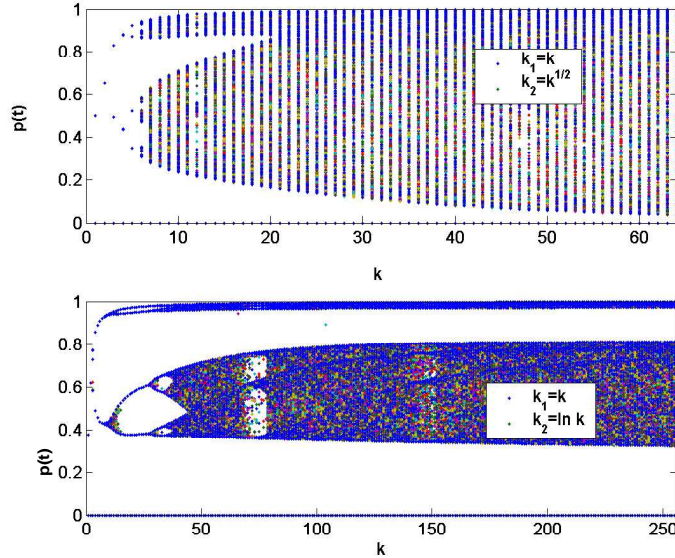
Figure 2. Bifurcation diagrams for the two dimensional map of the model (2.3). The two values for the number of parents are determined as functions of a parameter k graphed on the horizontal axis. In the first graph $k_1 = k, k_2 = \sqrt{k}$, while in the second graph, $k_1 = k, k_2 = \ln k$. In both graphs the proportion of nodes having k_1 parents is $\frac{M_1}{N} = \frac{3}{4}$, and the proportion of nodes having k_2 parents is $\frac{M_2}{N} = \frac{1}{4}$.

We now turn to a more extensive analysis of the map dynamics which will vividly illustrate the reverse bifurcations which we discuss in the next section. To this aim we first study the sensitivity of the orbits to the initial values. We consider the case of only two distinct values for the number of parents for simplicity. We fix the parameters $\frac{M_1}{N}, \frac{M_2}{N}, k_1, k_2$, and choose two initial pairs $(p_1(0), p_2(0))$ and $(q_1(0), q_2(0))$ as starting points for the orbits. We iterate many times the equations of the model and compute $p(t) = p_1(t) + p_2(t)$ and $q(t) = q_1(t) + q_2(t)$ for each time point t. Then we plot the error $E(t) = |p(t) - q(t)|$ versus t. In Figure 3 we show the case of $\frac{M_1}{N} = \frac{M_2}{N} = \frac{1}{2}, k_1 = 5$ and $k_2 = 3, 4, 95$, and 100 respectively, for illustration of the error behavior as k_2 increases. In all these graphs $p(0) = 0.5$ and

$q(0) = 0.5002$, so the starting values are very close. For values of k_2 smaller than 3 or larger than 100 the graphs are similar to the one for $k_2 = 3$.
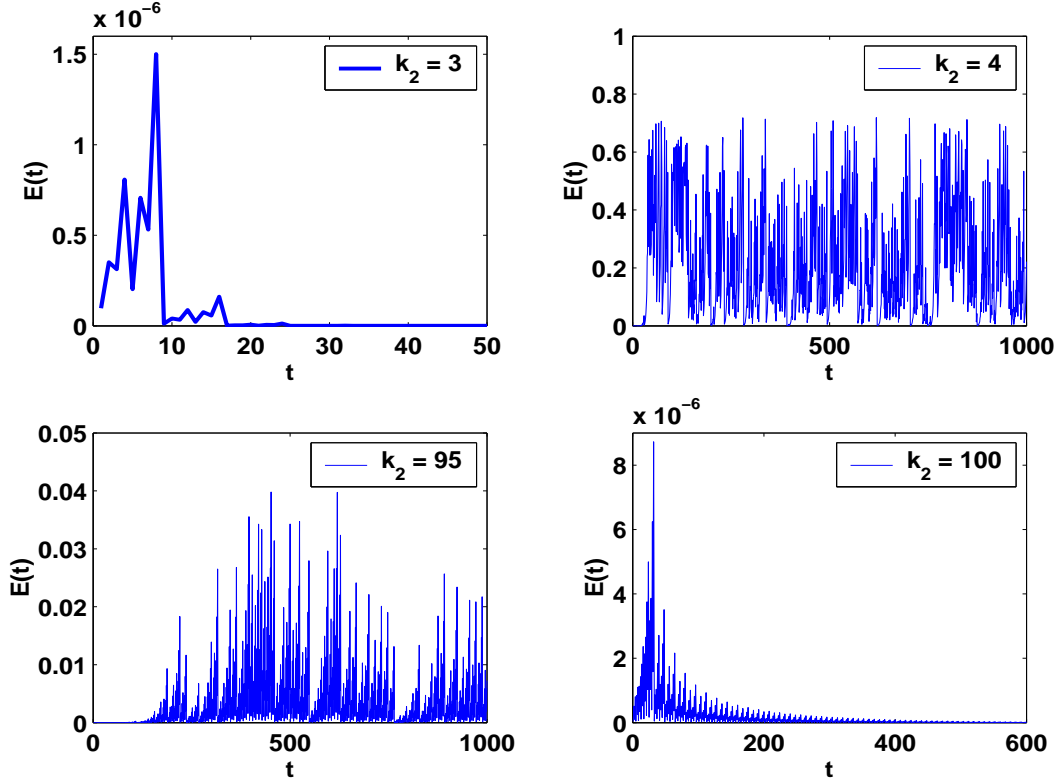

FIGURE 3. Sensitivity of the orbits to the initial values. The following parameters are fixed in each graph: $\frac{M_1}{N} = \frac{1}{2}, \frac{M_2}{N} = \frac{1}{2}, k_1 = 5, k_2 = 3, 4, 95$, and 100 respectively. Two initial pairs $(p_1(0), p_2(0))$ and $(q_1(0), q_2(0))$ are chosen as starting points for the orbits. The equations of the model are iterated and the values $p(t) = p_1(t) + p_2(t)$ and $q(t) = q_1(t) + q_2(t)$ are computed for each time point t. Then the error $E(t) = |p(t) - q(t)|$ is plotted versus t. In all these graphs $p(0) = 0.5$ and $q(0) = 0.5002$, so the starting values are very close. In each graph the scale is chosen for clarity purposes. For values of k_2 smaller than 3 or larger than 100 the graphs are similar to the one for $k_2 = 3$.

The range of t is not necessarily the same for all the graphs, but it is chosen so that one can see easily the behavior.

The results are similar for any choice of the fixed parameters and initial values. The authors have checked the behavior in tens of cases. In general, we observe that for small values of k_2 the error converges to zero. For larger values of k_2 the error does not settle suggesting that the initial perturbations propagate across the entire system which exhibits a chaotic behavior. In most cases, for k_2 very large the error converges to 0 again. The rate of convergence to zero may differ from one case to another. This suggests that the chaos is transient and the larger the k_2 the more likely it is that the system will become insensitive

to initial perturbations and will exhibit an ordered behavior. The range of k_2 corresponding to chaos changes from case to case, and depends on the parameter values. In general, the range becomes larger as k_1 increases. In the case illustrated here this range for k_2 is the interval $[4, 95]$ (we only show the cases of $k_2 = 4$ and $k_2 = 95$ in Figure 3. For all the other values in this interval the graphs are similar.).

These sensitivity graphs showing little sensitivity for small k_2 or large k_2, are consistent with the bifurcation diagrams to follow. Similar graphs and behavior are noticed also for cases with more than two distinct values for the number of parents.

In order to clarify even more the situation suggested by the sensitivity of the orbits to the initial values, we construct bifurcation diagrams with integer values for the parameters k. We consider the two dimensional case and fix the parameters $\frac{M_1}{N}, \frac{M_2}{N}$. It is important to observe that the model depends on M_1, M_2, and N only through the proportions $\frac{M_1}{N}, \frac{M_2}{N}$, representing the fraction of nodes having k_1 or k_2 parents. In Figure 4 we graph bifurcation maps for $\frac{M_1}{N} = \frac{M_2}{N} = \frac{1}{2}, k_1 = 1, 2, 3, 4, 5$ and let k_2 increase freely. Thus the diagrams represent p vs. (k_1, k_2) for only a few values of k_1, which allows one to understand how the diagrams change from one value of k_1 to another. We note here that the initial values (p_1, p_2) are the same for all the "slices" shown in the graph. In these diagrams k_2 is the parameter that increases freely, and given the fact that only the proportions $\frac{M_1}{N}, \frac{M_2}{N}$ matter, not the actual number of nodes, one can allow a wide range of values for the free parameter. One can observe that as k_1 increases from 1 to 5 period-doubling bifurcations occur and the map exhibits chaos. However, when looking at, for example, slices $k_1 = 4$ and $k_1 = 5$ one can see that the bifurcation is reversed as k_2 becomes larger, and the point where the bifurcation is reversed is shifted to the right on the k_2 axis.

For more clarity we attach the two dimensional slice for $k_1 = 5$ in the first graph of Figure 5. The graph is over a significantly wider range of k_2 values than the three dimensional graph. The bifurcation is reversed around $k_2 = 10$ when $k_1 = 4$, around $k_2 = 25$ when $k_1 = 5$, and around $k_2 = 1100$ when $k_1 = 10$ (not shown). Other than that, the graphs are similar. So it is observed that as k_1 increases the point of reversed bifurcation moves towards ∞ when graphing the bifurcation diagrams for p vs k_2. In the second graph of Figure 5 we provide a zoom in on a small range of k_2 values for $k_1 = 5$, to see that the route to chaos is due to a cascade of period-doubling bifurcations. This process is reversed for large k_2 values. We note here that this situation is similar as k_1 takes values beyond the ones shown in the figures.

On the other hand, if one looks at a fixed k_1 and changes the proportion $\frac{M_1}{N}$ (that is the proportion of nodes having k_1 parents) the same thing happens; the reversed bifurcation occurs for larger values of k_2 as the proportion gets larger. However, the graphs are similar in shape with any of the other ones presented here. Similar situations are obtained for more than two distinct values of k.

Thus the bifurcation diagrams emphasize the situation observed in the error plot. The system exhibits chaotic behavior due to period-doubling bifurcations as one parameter is fixed and the other one increases
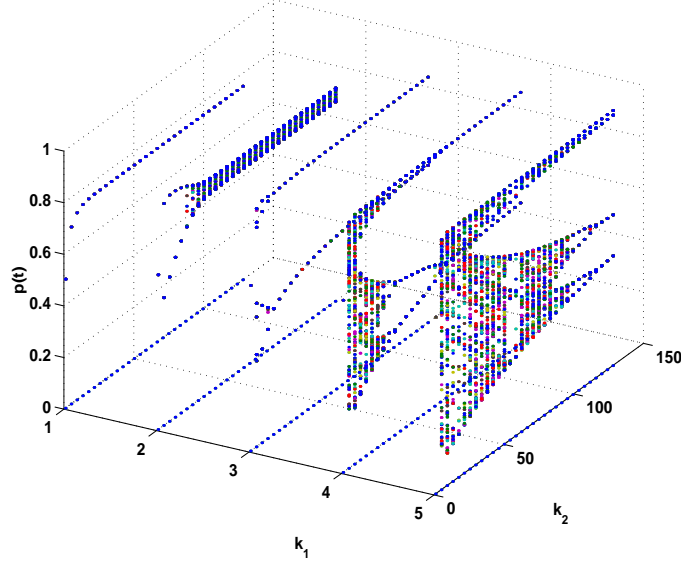
FIGURE 4. Bifurcation diagrams for $k_1 = 1, 2, 3, 4, 5$ graphed as functions of k_2. The proportions of nodes with k_1 and k_2 parents are equal, that is $\frac{M_1}{N} = \frac{M_2}{N} = \frac{1}{2}$. The equations of the model are iterated 100 times to eliminate any transient behavior. As k_1 increases from 1 to 5 period-doubling bifurcations occur and the map exhibits chaos. For $k_1 = 4, 5$ the bifurcations are reversed, and the point of reversed bifurcations occurs for larger k_2 as k_1 increases.

to ∞. However, for larger values of the free parameter the chaos is reversed through a cascade of period-halving bifurcations. Reverse bifurcations are discussed in Section 4.

To complete the study of the dynamics of the model, we consider also the fixed points of the maps (2.4), by solving the system

$$(3.1) \qquad p_i = \frac{M_i}{N} \left[1 - \left(1 - \sum_{j=1}^{J} p_j \right)^{k_i} + \frac{p_i}{\frac{M_i}{N}} \left(\left(1 - \sum_{j=1}^{J} p_j \right)^{k_i} - \left(\sum_{j=1}^{J} p_j \right)^{k_i} \right) \right]$$

where $i = 1, 2, \ldots, J$. Of course, we do this numerically for various parameters. In what follows we provide for illustration the case $\frac{M_1}{N} = \frac{M_2}{N} = \frac{1}{2}, k_1 = 1, 4$, letting k_2 free (so $J = 2$). The first two graphs in Figure 6 provide the fixed points (p_1, p_2) vs. k_2. We observe that $p_1 \to \frac{1}{4}$, and $p_2 \to \frac{1}{2}$. The rate of convergence is slower for larger k_1. Due to the complexity of the computations for large powers k we could only graph 30 values of k_2 in the case $k_1 = 4$, but it is apparent from the graph that for $k_2 \to \infty$ the fixed points converge to the specified values.

We rewrite the equations (3.1) as follows

$$(3.2) \qquad p_i = \frac{\frac{M_i}{N} \left[1 - \left(1 - \sum_{j=1}^{J} p_j \right)^{k_i} \right]}{1 - \left(1 - \sum_{j=1}^{J} p_j \right)^{k_i} + \left(\sum_{j=1}^{J} p_j \right)^{k_i}}.$$
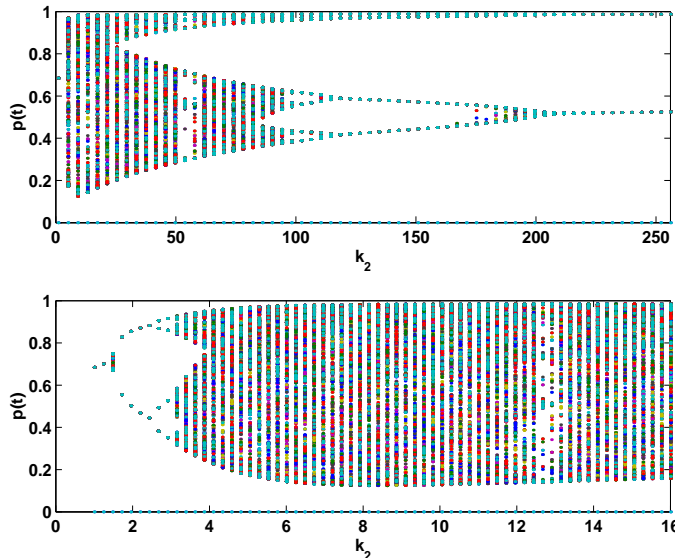
FIGURE 5. Bifurcation diagrams for $k_1 = 5$ in more detail. The proportions of nodes with k_1 and k_2 parents are equal, that is $\frac{M_1}{N} = \frac{M_2}{N} = \frac{1}{2}$. The first graph indicates that the chaotic behavior is reversed through a cascade of period-halving bifurcations, while the second graph shows that the map exhibits chaos through a cascade of period-doubling bifurcations. The second graph is a zoom-in on the first graph over a small range of k_2 values. Similar graphs are obtained for other values of k_1.

Observe that if $k_i = 1$ the equation can be solved and $p_i = \frac{1}{2} \cdot \frac{M_i}{N}$. This means that for the illustrated case of $\frac{M_1}{N} = \frac{1}{2}$, we get $p_1 = \frac{1}{4}$, which is clearly shown in Figure 6. Also, if in the right term of (3.2) we let $k_i \to \infty$, assuming all the other quantities fixed, we get $p_i \to \frac{M_i}{N}$. This coincides with our simulation result in Figure 6 of $p_2 \to \frac{1}{2}$. To illustrate this even better we generate the simulation of fixed points for the case of three distinct number of parents and fix $\frac{M_1}{N} = 0.3, \frac{M_2}{N} = 0.6, \frac{M_3}{N} = 0.1, k_1 = 1$, and $k_2 = 1$ and let k_3 move freely, we obtain that $p_1 = 0.15, p_2 = 0.3, p_3 \to 0.1$, shown in the last graph of Figure 6.

Figure 6 corresponds to figure 2 (bottom) in [5].

We make the remark that in the previous simulations we studied mainly cases with only two distinct values for the number of parents. However, the conclusions hold for other cases with more than two values for the number of parents, and have been checked by the authors through numerous simulations.

4. REVERSE BIFURCATIONS

It was shown in the last section that by holding k_1 fixed and letting k_2 increase in the two dimensional model, a sequence of reversed bifurcations occurs. Before examining the phenomenon more closely, it is useful to examine reverse bifurcations in a more general way.
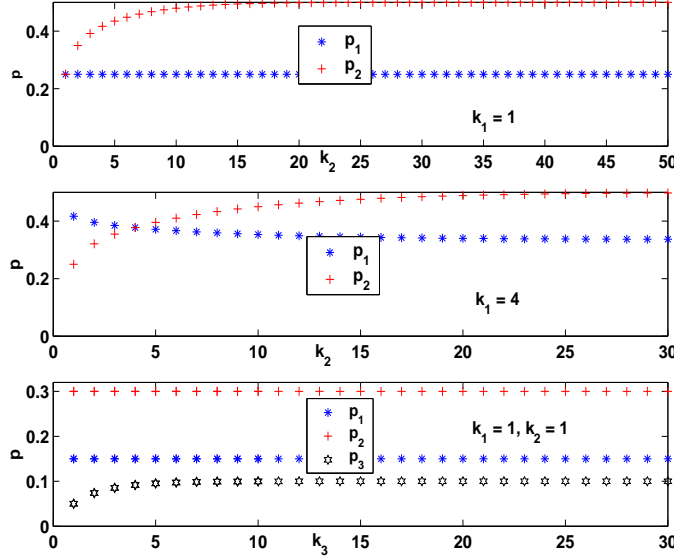
FIGURE 6. Fixed points of the maps (2.4) obtained numerically by solving the system (3.1). The first two graphs illustrate the case $\frac{M_1}{N} = \frac{M_2}{N} = \frac{1}{2}, k_1 = 1$, and 4 respectively, letting k_2 free. The third graph illustrates the case $\frac{M_1}{N} = 0.3, \frac{M_2}{N} = 0.6, \frac{M_3}{N} = 0.1, k_1 = 1, k_2 = 1$, and k_3 moving freely. The convergence of the p's to the values obtained by the equation (3.2) are apparent from the graphs.

The familiar one dimensional quadratic map

$$x_{n+1} = ax_n(1 - x_n)$$

has only period doubling bifurcations on $0 \le a \le 4$. However, replacing the linear parameter a by the tent shaped parameter $4 - |a - 4|, 0 \le a \le 8$, gives the map

$$x_{n+1} = (4 - |a - 4|) x_n(1 - x_n),$$

which leads to a bifurcation diagram on $0 \le a \le 8$ extended by mirror symmetry as in Figure 7.

However, it is possible to have a period halving bifurcation sequence in a one dimensional unimodal (one-hump) map even with the parameter appearing as linear multiplier ([27], [33], [34]). Alternately, relaxing the unimodality can also introduce reverse bifurcation sequence ([17]). These papers suggest and even provide a rough outline for a general theory of when reverse bifurcations will appear in one dimensional maps.

Not surprisingly the situation is much more complicated for multidimensional maps. It has been observed that the two dimensional Henon map does have both orbit creation and orbit annihilation parameter values ([23]). In fact these authors give a very general result for dissipative maps of the plane into itself. However most specific examples discussed in the literature are neither conservative nor dissipative ([12], [28], [36], [39]).
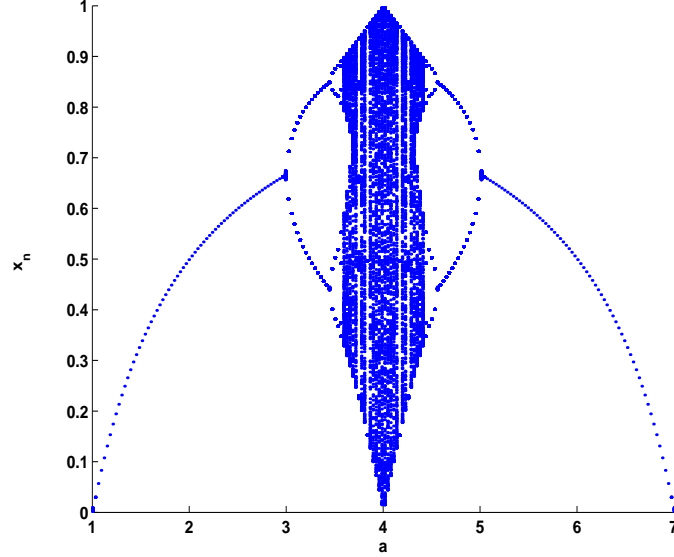
FIGURE 7. Bifurcation diagram for the one dimensional map $x_{n+1} = (4 - |a - 4|) \, x_n (1 - x_n)$. A cascade of period doubling bifurcations is followed by a cascade of period halving bifurcations.

The easiest way to understand the appearance of reverse bifurcations in our generalization of the Andrecut and Ali map [5] is to consider the two dimensional case, that is with two distinct k values, k_1 and k_2, and take the limit as $k_2 \to \infty$ in the expressions for p_1 and p_2

$$(4.1) \quad p_1(t+1) = \frac{M_1}{N}\left[1 - (1 - p_1(t) - p_2(t))^{k_1} + \frac{p_1(t)}{\frac{M_1}{N}}\left((1 - p_1(t) - p_2(t))^{k_1} - (p_1(t) + p_2(t))^{k_1}\right)\right]$$

$$p_2(t+1) = \frac{M_2}{N}\left[1 - (1 - p_1(t) - p_2(t))^{k_2} + \frac{p_2(t)}{\frac{M_2}{N}}\left((1 - p_1(t) - p_2(t))^{k_2} - (p_1(t) + p_2(t))^{k_2}\right)\right]$$

to obtain (with all the other variables and parameters held fixed)

$$p_2(t+1) = \frac{M_2}{N}.$$

It is assumed here that $p_1(t) + p_2(t)$ is bounded away from zero, justified because $(0,0)$ is an unstable equilibrium point for (4.1).

Assuming again for simplicity that $\frac{M_1}{N} = \frac{M_2}{N} = \frac{1}{2}$, we can take $p_2(t) = \frac{1}{2}$ and (4.1) becomes

$$(4.2) \qquad p_1(t+1) = \frac{1}{2} - \left(\frac{1}{2} - p_1(t)\right)^{k_1+1} - p_1(t)\left(\frac{1}{2} + p_1(t)\right)^{k_1}$$

$$p_2(t+1) = \frac{1}{2}$$

as $k_2 \to \infty$. Or, with $p = p_1 + p_2$,

$$(4.3) \qquad p(t+1) = p_1(t+1) + p_2(t+1) = 1 - (1 - p(t))^{k_1+1} - \left(p(t) - \frac{1}{2}\right)p(t)^{k_1}.$$

This map represents the behavior for large k_2 of the three dimensional bifurcation diagram in Figure 4 of the previous section.

But the limiting behavior can also be described by the bifurcation diagram of the map (4.3) itself as in Figure 8. Thus, for $0 \leq k_1 \leq 2$ there is a single stable fixed point and for $k_1 > 2$ a single stable period two orbit. This is, of course, exactly what shows up in the two dimensional bifurcation diagram for (k_2, p) for different values of k_1 (Figure 5).
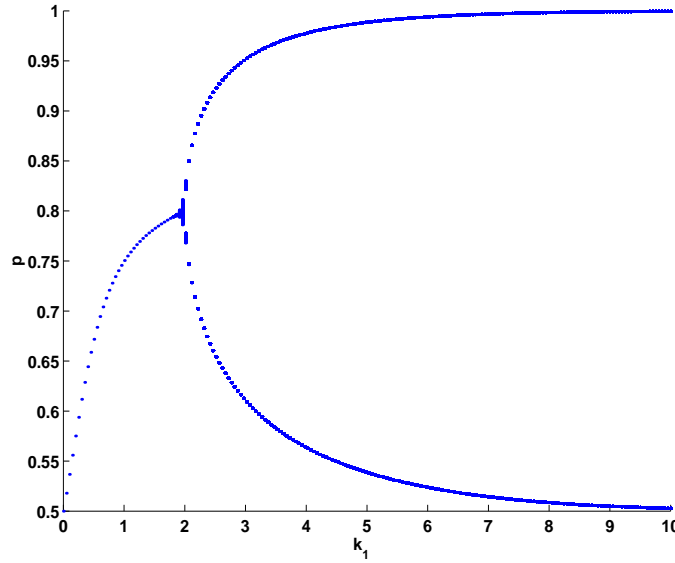

FIGURE 8. Bifurcation diagram for the map $p(t+1) = 1 - (1 - p(t))^{k_1+1} - p(t) - \frac{1}{2} p(t)^{k_1}$.

It is also of interest to look at the reduced map (4.2) directly, but now simplified by removing $p_2(t+1) = \frac{1}{2}$ and $k_2 \to \infty$ by viewing it entirely as a map for p_1 with a single parameter k_1 as in the first equation of (4.2). This map is viewed first as a surface $p_1(t+1)$ vs. $(p_1(t), k_1)$ as in the first graph of Figure 9.

Now, the graph of the map (4.2) itself (with $k_1 = 5$) and its first six iterates show that the higher iterates introduce essentially no new complexity and therefore only the simplest periodic, and no chaotic, behavior is observed (Figure 10). Of course, the bifurcation diagram for $(p_1(t), k_1)$ is that of $(p(t), k_1)$ reduced by $\frac{1}{2}$.

We now show that a similar phenomenon occurs in higher dimensions than two. Start with the 3 dimensional system:

$$p_1(t+1) = \frac{M_1}{N} \left[1 - (1 - p_1 - p_2 - p_3)^{k_1} \right] + p_1 \left[(1 - p_1 - p_2 - p_3)^{k_1} - (p_1 + p_2 + p_3)^{k_1} \right]$$

$$p_2(t+1) = \frac{M_2}{N} \left[1 - (1 - p_1 - p_2 - p_3)^{k_2} \right] + p_2 \left[(1 - p_1 - p_2 - p_3)^{k_2} - (p_1 + p_2 + p_3)^{k_2} \right]$$

$$p_3(t+1) = \frac{M_3}{N} \left[1 - (1 - p_1 - p_2 - p_3)^{k_3} \right] + p_3 \left[(1 - p_1 - p_2 - p_3)^{k_3} - (p_1 + p_2 + p_3)^{k_3} \right].$$
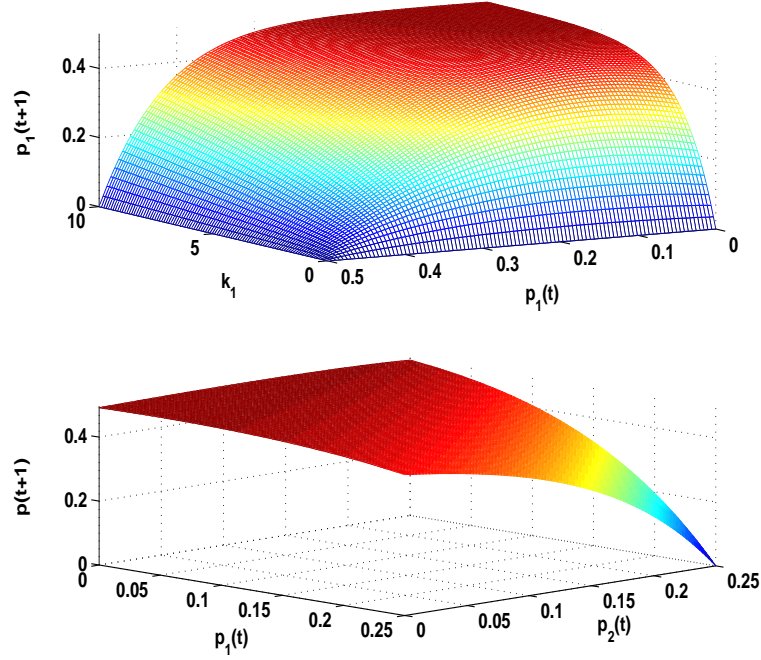
FIGURE 9. The first graph represents the surface map for $p_1(t+1)$ vs $(k_1, p_1(t))$ from (4.2), $p_1(t+1) = \frac{1}{2} - \left(\frac{1}{2} - p_1(t)\right)^{k_1+1} - p_1(t)\left(\frac{1}{2} + p_1(t)\right)^{k_1}$. The second graph represents $p_1(t+1)$ vs $(p_1(t), p_2(t))$ from (4.4), $p_1(t+1) = \frac{1}{4} + \left(p_1 - \frac{1}{4}\right)\left(\frac{1}{2} - p_1 - p_2\right)^{k_1} - p_1\left(\frac{1}{2} + p_1 + p_2\right)^{k_1}$, $p_2(t+1) = \frac{1}{4} + \left(p_2 - \frac{1}{4}\right)\left(\frac{1}{2} - p_1 - p_2\right)^{k_2} - p_2\left(\frac{1}{2} + p_1 + p_2\right)^{k_2}$.

Taking $\frac{M_1}{N} = \frac{M_2}{N} = \frac{1}{4}$ and $\frac{M_3}{N} = \frac{1}{2}$ for simplicity and letting $k_3 \to \infty$, we obtain $p_3(t) \equiv \frac{1}{2}$. Then the first two equations can be simplified to obtain

$$(4.4) \qquad p_1(t+1) = \frac{1}{4} + \left(p_1 - \frac{1}{4}\right)\left(\frac{1}{2} - p_1 - p_2\right)^{k_1} - p_1\left(\frac{1}{2} + p_1 + p_2\right)^{k_1}$$

$$p_2(t+1) = \frac{1}{4} + \left(p_2 - \frac{1}{4}\right)\left(\frac{1}{2} - p_1 - p_2\right)^{k_2} - p_2\left(\frac{1}{2} + p_1 + p_2\right)^{k_2}.$$

Then

$$p(t+1) = p_1(t+1) + p_2(t+1)$$

produces a monotone graph ($k_1 = 5, k_2 = 10$ for definiteness) as in the second part of Figure 9 similar to the one dimensional case (first graph in Figure 9).

By analogy with the two dimensional case, this shows that a very high connectivity value k for even one of the classes of nodes swamps out any possible chaos in the network and results in only the simplest steady state or period two behavior for the entire system.
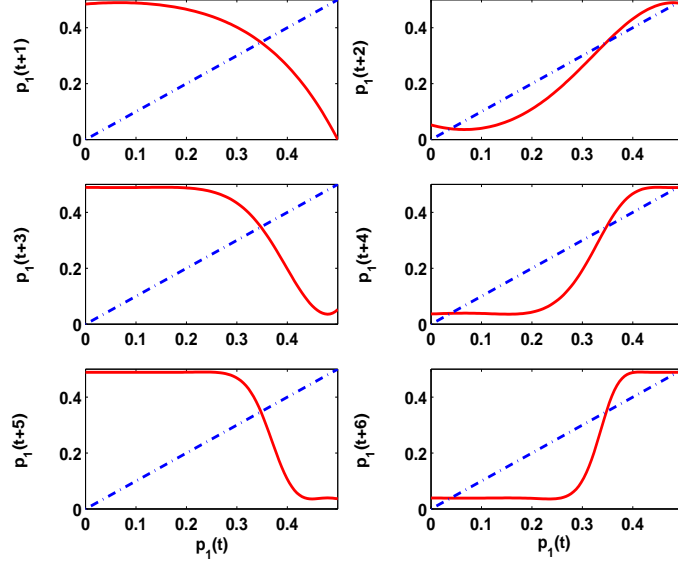
FIGURE 10. The first 6 iterates of the map (4.2), $p_1(t+1) = \frac{1}{2} - \left(\frac{1}{2} - p_1(t)\right)^{k_1+1} - p_1(t)\left(\frac{1}{2} + p_1(t)\right)^{k_1}$. Here $k_1 = 5$.

5. Conclusions

The original motivation for the probability density equation (2.1) is that it generalizes the elementary cellular automata rule 126. Rule 126 says that a node is turned off if and only if its precursors are either all on or all are off. If a more general one-dimensional periodic cellular automata is set up in the same manner, each node being turned off if and only if each of its k (constant) nearest neighbors are all on or all off, then it is easy to show that its density function either approaches a limiting value or a period two orbit. This is exactly the behavior exhibited in Figure 8 for random Boolean networks. We have just shown that if a network is operating under a generalized rule 126 and one segment of nodes has a very large set of precursors, then the rest of the network, at least in toto, has a greatly simplified behavior (at most two different modes).

This paper generalizes a cellular automaton model proposed in [5] for a Boolean network with a unique Boolean rule for all nodes. The number of parents of a node is considered fixed in the earlier paper, while in this paper we allow for a variable number of parents for each node. The model proposed is a natural extension of the one in [5] and it is shown that in the particular case when all nodes have the same number of parents, the model coincides with theirs. An algorithm for the simulation of the model is introduced and simulation results show that the model fits the real Boolean system well. The dynamics of the model show that the route to chaos is due to a cascade of period-doubling bifurcations, followed by a cascade of period-halving bifurcations.

It would be of interest to continue the study of this model under the assumption of a power-law distribution of the number of parents of the nodes, in light of the recent studies on scale-free networks ([1], [2], [3], [6]). Under such an assumption, the number of parents is chosen randomly from a distribution with a probability distribution function of the type

$$P_\gamma(k) = \frac{1}{\zeta(\gamma, N)\, k^\gamma}, \qquad k = 1, 2, \ldots, N$$

where N is the network size, $\zeta(\gamma, N) = \sum_{k=1}^{N} \frac{1}{k^\gamma}$ is the incomplete Riemann Zeta function, and γ is a parameter whose values have a heavy influence on the behavior of the system (see [1], [2], or [6] for example). Analyzing the attractors and the basins of attraction would be of great interest, as well as the transient time to reach an attractor. Also, introducing "noise" in the system would allow one to study the stability of the system to perturbations. In scale-free networks perturbing a very highly connected node is expected to have a much bigger impact than perturbing a node with low connectivity.

Another topic for further investigations is to consider an asynchronous update of the Boolean rule, since this is of importance in modeling systems composed of multiple interacting components. For example, in certain biological systems, an ordered asynchronous (OAS) state update has a role in emergent modularity, which in turn may contribute to the formation of dynamical hierarchies in these biological systems ([7], [11]). It will be interesting to look at four different types of updating schemes, namely the clock scheme ([26], [35]), the cyclic scheme ([24]), the random independent scheme ([18]), and the random order scheme ([18]). It has been shown ([11]) that properties of the models are changed by the particular update scheme chosen.

It would also be of interest to go one step further in this paper's generalization and allow for multiple Boolean rules to be used in the iterations of the system, thus surpassing the case of cellular automata. This would require a change in the approach, given that the Boolean rule was heavily used in generating the model. On the other hand, only changing the unique Boolean rule to be used based on other cellular automata rules ([38]) could lead to interesting new models and dynamic behaviors. The area of exploration is wide open.

References

[1] Albert R., Barabasi A-L., *Dynamics of complex systems: scaling laws for the period of Boolean networks*, Physical Review Letters, 84, 24 (2000), p. 5660-5663.

[2] Aldana M., *Boolean dynamics of networks with scale-free topology*, Physica D, 185 (2003), p. 45-66.

[3] Aldana M., Cluzel P., *A natural class of robust networks*, PNAS, 100, 15 (2003), p. 8710-8714.

[4] Alligood K. T., Sauer T. D., Yorke J. A., *Chaos, An introduction to dynamical systems*, Springer-Verlag New York, 1997, p. 533.

[5] Andrecut M., Ali M. K., *Chaos in a simple Boolean network*, International Journal of Modern Physics B, Vol. 15, 1 (2001), p. 17-23.

[6] Barabasi A-L., Albert R., Jeong H., *Mean-field theory for scale-free random networks*, Physica A, 272 (1999), p. 173-187.

[7] Bedau M.A., McCaskill J.S., Packard N.H., Rasmussen S., Adami C., Green D.G., Ikegami T., Kaneko K., Ray T.S., *Open problems in artificial life* , Artificial Life, 6 (2000), p. 363-376.

[8] Boccara N., Roblin O., Roger M., *Route to chaos for a global variable of a two-dimensional 'game-of-life' automata network*, Journal of Physics A: Math. Gen, 27 (1994), p. 8039-8047.

[9] Chopard B., Droz M., *Cellular automata modeling of physical systems*, Cambridge, 1998.

[10] Chua L.O., Yoon S., Dogaru R., *A nonlinear dynamics perspective of Wolfram's new kind of science. Part I: Threshold of Complexity*, International Journal of Bifurcation and Chaos, Vol. 12, 12 (2002), p. 2655-2766.

[11] Cornforth D., Green D.G., Newth D., Kirley M., *Do artificial ants march in step? Ordered asynchronous processes and modularity in biological systems* , Artificial Life VIII, MIT Press, 2002, p. 28-32.

[12] De Monte S., d'Ovidio F., Mosekilde E., *Noise-induced macroscopic bifurcation in populations of globally coupled maps*, cond-mat/0301056.

[13] Flyvbjerg H., Kjaer N.J., *Exact solution of Kauffman's model with connectivity one*, Journal of Physics A: Math. Gen., 21 (1988), p. 1695-1718.

[14] Fogelman-Soulie F., Goles-Chacc E., Weisbuch G., *Specific roles of the different Boolean mappings in random networks*, Bulletin of Mathematical Biology, Vol. 44, 5 (1982), p. 715-730.

[15] Fogelman-Soulie F., *Frustration and stability in random Boolean networks*, Discrete Applied Mathematics, 9 (1984), p. 139-156

[16] Fox J.J., Hill C.C., *From topology to dynamics in biochemical networks*, Chaos, Vol. 11, 4 (2001), p. 809-815.

[17] Frame M., Shontel M., *Reverse bifurcations in a quartic family* , Computers and Graphics, 24 (2000), p. 143-149.

[18] Harvey I., Bossomaier T., *Time out of joint: attactors in asynchronous random Boolean networks*, Proceedings of the Fourth European Conference on Artificial Life (ECAL97), MIT Press, 1997, p. 65-75.

[19] Heidel J., Maloney J., Farrow C., Rogers J.A., *Finding cycles in synchronous Boolean networks with applications to biochemical systems*, International Journal of Bifurcation and Chaos, 13 (2003), p. 535-552.

[20] Huang S., Ingber D.E., *Shape - dependent control of cell growth, differentiation, and apoptosis: switching between attractors in cell regulatory networks*, Experimental Cell Research, 261 (2000), p. 91-103.

[21] Huang S., *Genomics, complexity and drug discovery: insights from Boolean network models of cellular regulation*, Pharmacogenomics, 2, 3 (2001), p. 203-222.

[22] Huang S., *Regulation of Cellular States in Mammalian Cells from a genomwide view*, Gene Regulation and Metabolism, MIT Press, Cambridge, Massachusetts, London, England, p. 181-220.

[23] Kan I., Kocak H., Yorke J., *Anti-monotonicity: concurrent creation and annihilation of periodic orbits*, Annals of Mathematics, 136 (1992), p. 219-252.

[24] Kanada Y., *The effects of randomness in asynchronous 1D cellular automata*, Proceedings of ALIFE IV, 1994.

[25] Kauffman S.A., *The origins of order*, Oxford University Press, 1993, p. 173-235.

[26] Low S., Lapsley D., *Optimization flow control, i: Basic algorithm and convergence*, IEEE/ACM Transactions on Networking, 1999.

[27] Nusse H.E., Yorke J.A., *Period halving for $x_{n+1} = MF(x_n)$ where F has negative Schwarzian derivative*, Physics Letters A, 127 (1988), p. 328-334.

[28] Selgrade J.F., *Using stocking or harvesting to reverse period-doubling bifurcations in discrete population models*, Journal of Difference Equations and Applications, 4 (1998), p. 163-183.

[29] Sherlock R.A., *Analysis of the behaviour of Kauffman binary networks - I. State space description and the distribution of limit cycle lengths*, Bulletin of Mathematical Biology, Vol. 41 (1979), p. 687-705.

[30] Silvescu A., Honavar V., *Temporal Boolean network models of genetic networks and their inference from gene expression time series*, Complex Systems, 13 (2001), p. 61-78.

[31] Shmulevich I., Dougherty E.R., Kim S., Zhang W., *Probabilistic Boolean networks: a rule-based uncertainty model for gene regulatory networks*, Bioinformatics, Vol. 18, 2 (2002), p. 261-274.

[32] Stauffer D., *Percolation thresholds in square-lattice Kauffman model*, Journal of Theoretical Biology, 135 (1988), p. 255-261.

[33] Stone L. *Period-doubling reversals and chaos in simple ecological models*, Nature, 365 (1993), p. 617-620.

[34] Stone L., Hart D., *Effects of immigration of the dynamics of simple population models*, Theoretical Population Biology, 55 (1999), p. 227-234.

[35] Thomas R., ed., *Kinetic Logic: A Boolean approach to the analysis of complex regulatory systems*, Lecture Notes in Biomathematics, Springer Verlag, 29 (1979).

[36] Williams R.J., Martinez N.D., *Stabilization of chaotic and non-permanent food web dynamics*, preprint, 2001.

[37] Wolfram S., *Statistical mechanics of cellular automata*, Rev. Mod. Physics, 55 (1983), p. 601.

[38] Wolfram S., *A new kind of science*, Wolfram Media, Champaign, 2002, p. 51-114.

[39] Zhang X., Jarrett D.F., *Chaos in a dynamic model of traffic flows in an origin-destination network*, Chaos, 8 (1998), p. 503-513.